Supporting Information

Anionic F Doping-Induced Engineering of P2-Type Layered Cathode Materials for High-Performance Potassium-Ion Batteries

Yurong Wu, [a,b] Ziyun Zhang, [a,b] Jiangshan Huo, [a,b] Runguo Zheng, [a,b,c] Zhishuang Song, [a,b,c] Zhiyuan Wang, *[a,b,c] Yanguo Liu, [a,b,c] Dan Wang, [a,b,c]

a School of Materials Science and Engineering, Northeastern University, Shenyang 110819, P.R. China;

b School of Resources and Materials, Northeastern University at Qinhuangdao, Qinhuangdao 066004, P.R.China;

c Key Laboratory of Dielectric and Electrolyte Functional Material Hebei Province, Qinhuangdao, P.R.China;

*Corresponding author, (Zhiyuan Wang), zhiyuanwang@neuq.edu.cn;

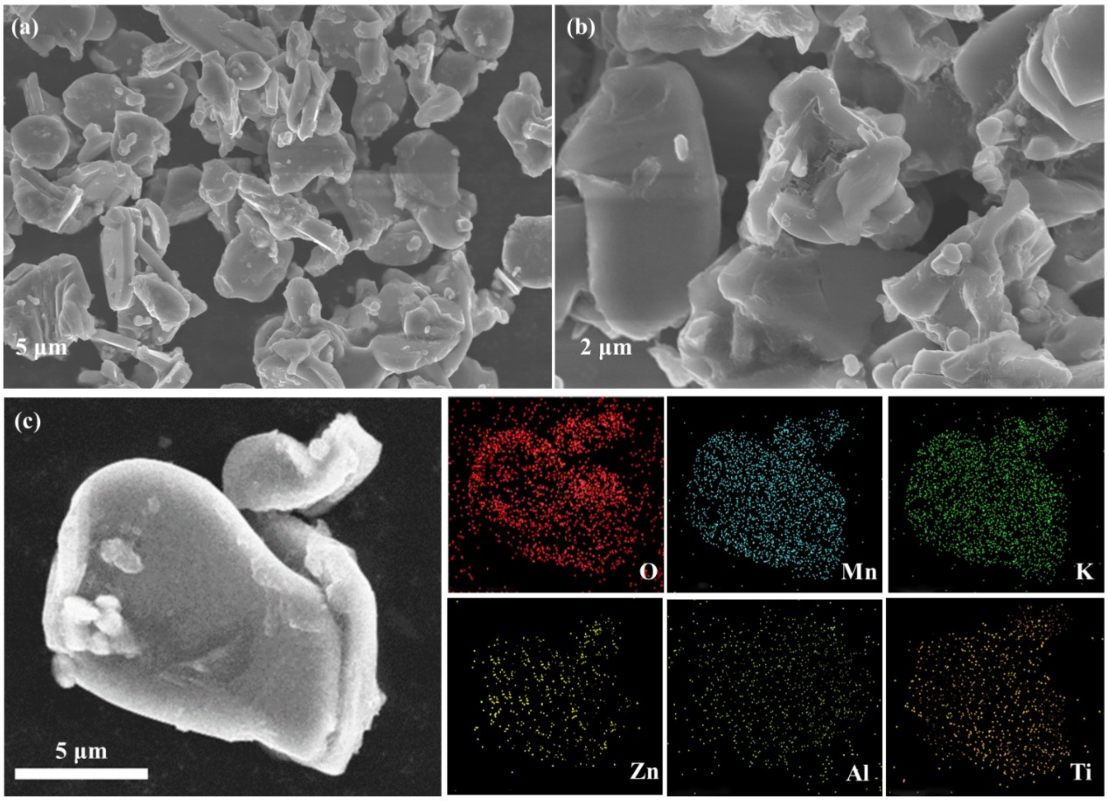

Fig. S1 The SEM images of KTMO powder cathode materials, and corresponding to EDS mappings, detection elements include K, Mn, Zn, Ti, Al, and O, respectively.

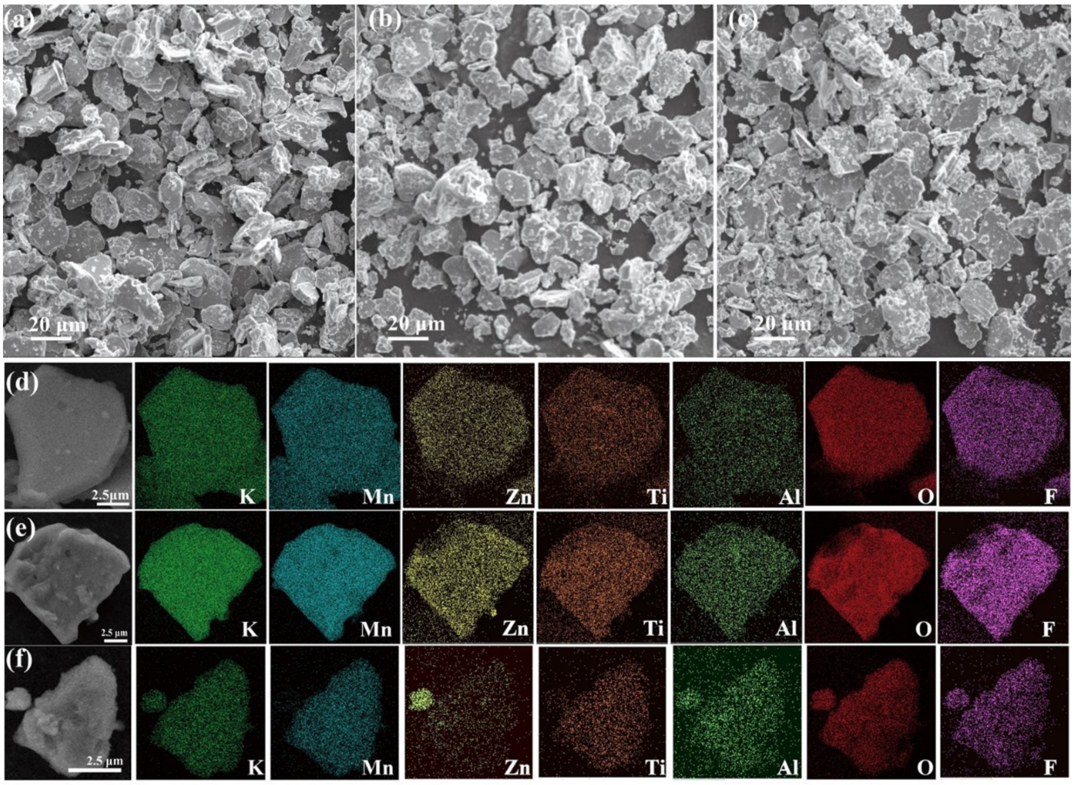

Fig. S2 The SEM images of (a) KTMO-F5, (b) KTMO-F7, and (c) KTMO-F10 powder cathode materials, and corresponding to EDS mappings, detection elements include K, Mn, Zn, Ti, Al, O, and F, respectively.

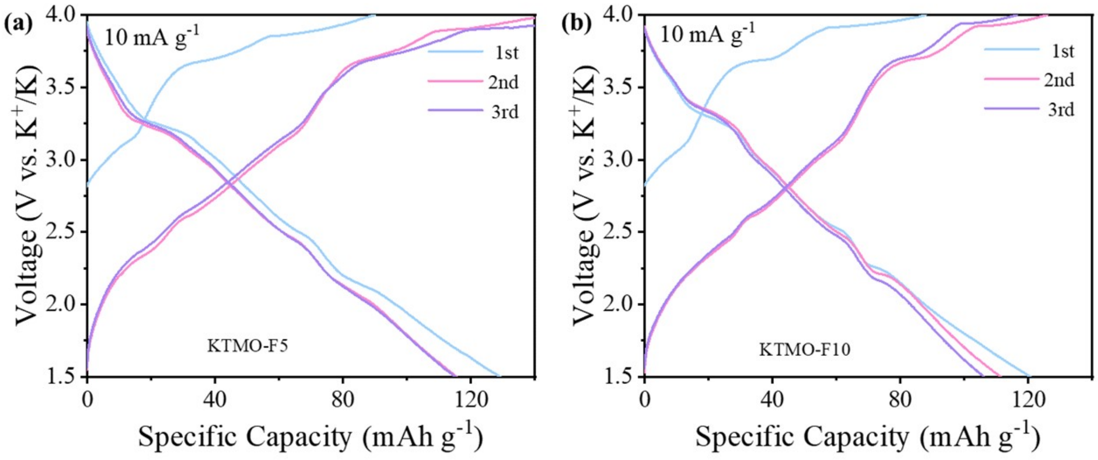

Fig. S3 The charge and discharge curves of the (a) KTMO-F5 and (b) KTMO-F10.

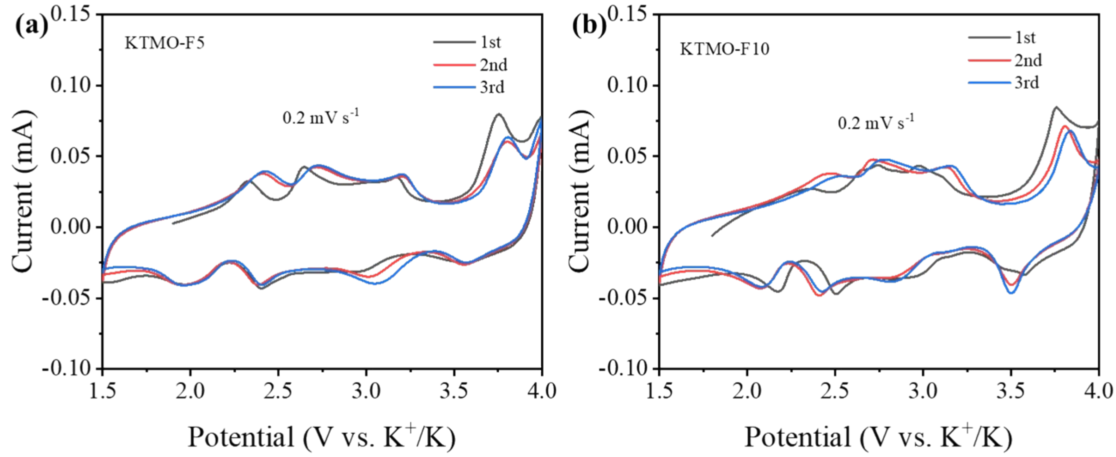

Fig. S4 The CV curves for the first three of the (a) KTMO-F5 and (b) KTMO-F10.

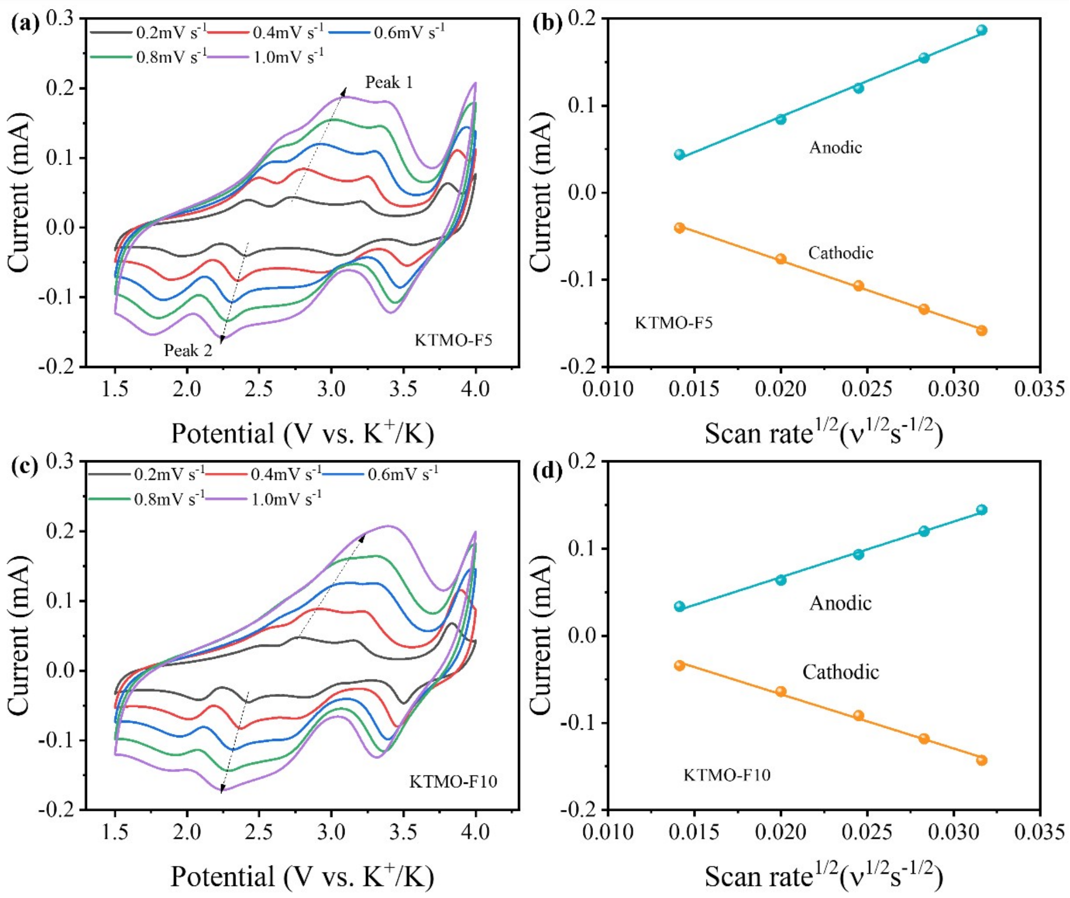

Fig. S5 CV curves and the linear fitting of peak current with the square root of sweeping rates ($\upsilon^{1/2}$) of (a, b) KTMO-F5 and (c, d) KTMO-F10.

CV curves of the P2-KTMO electrode cycled between 1.5 and 4.0 V at different scan rates. Figure S5 represents the linear relationship between the peak currents and the square root of sweep rates ($v^{1/2}$); the aligned fitting results suggest that the electrochemical K^+ (de)intercalation reactions are diffusion-controlled processes. Therefore, K^+ apparent diffusion coefficient was calculated according to the Randles-Sevcik Equation as:

$$I_p = 269000 n^{3/2} A C D^{1/2} v^{1/2}$$

In this equation, n represents the number of electrons per reaction species, A is the contact area between electrode and electrolyte, C is the concentration of K^+ in the lattice, D is the diffusion coefficient of K^+. They are calculated to be 1.534×10^{-11} cm^2 s^{-1} for KTMO-F5, 9.18×10^{-12} cm^2 s^{-1} for KTMO-F10.

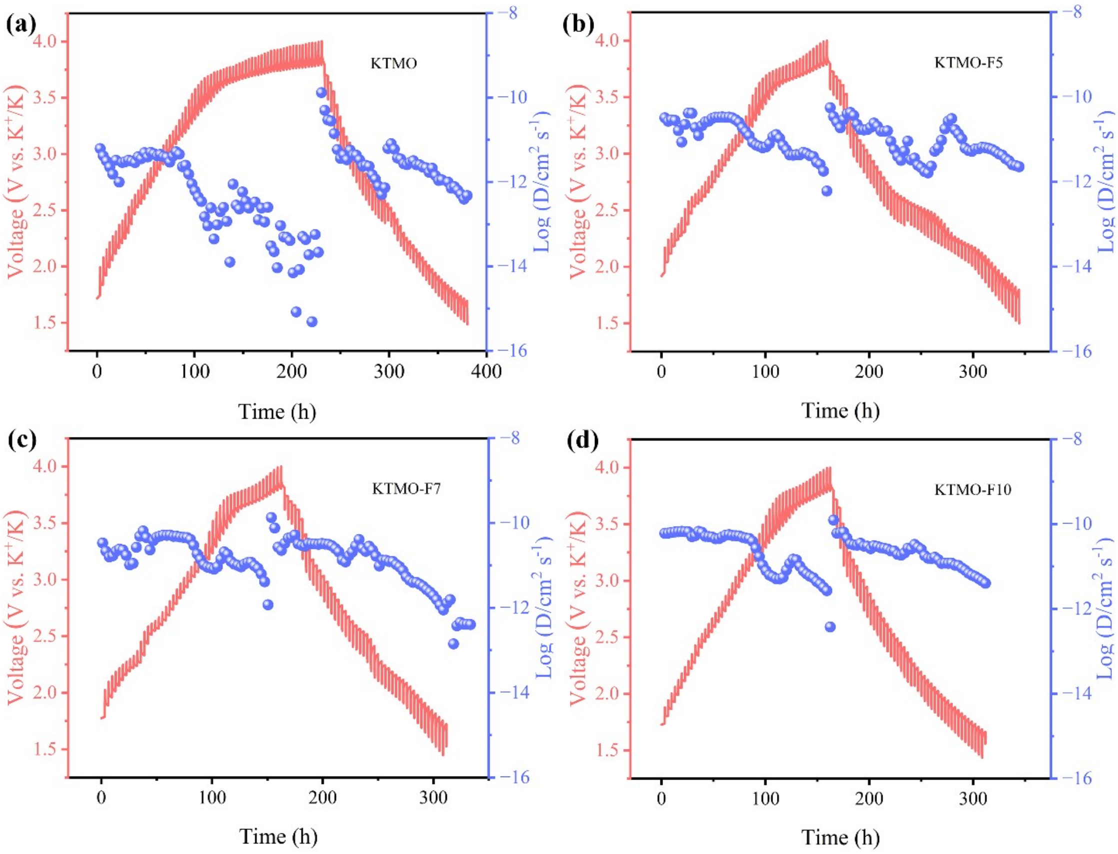

Fig. S6 Galvanostatic charge/discharge profiles and K^+ diffusivity coefficient of (a) KTMO, (b) KTMO-F5, (c) KTMO-F7, and (d) KTMO-F10.

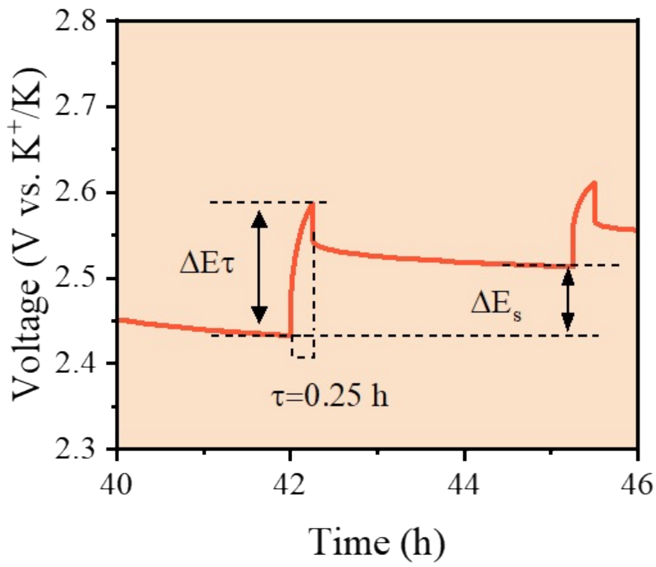

Fig. S7 Current step diagrams of KTMO-F7 at 2.45 V in charge process.

Galvanostatic intermittence titration technique (GITT) technique was used to calculate the K^+ diffusivity coefficient reflecting the kinetic behavior of KTMO and the K^+ diffusivity coefficient was calculated based on equation:

$$D_{K^+} = \frac{4}{\pi\tau}\left(\frac{m_B V_m}{M_B S}\right)^2\left(\frac{\Delta E_s}{\Delta E_\tau}\right)^2$$

In this equitation, m_B is the mass of the active materials, V_m is the molar volume, M_B is the molecular weight, S is the contact area between electrode and electrolyte, and ΔEs is the difference of the steady-state voltage of cell for the rest, $\Delta E\tau$ is the total transient voltage difference of the cell for applied current for time τ.

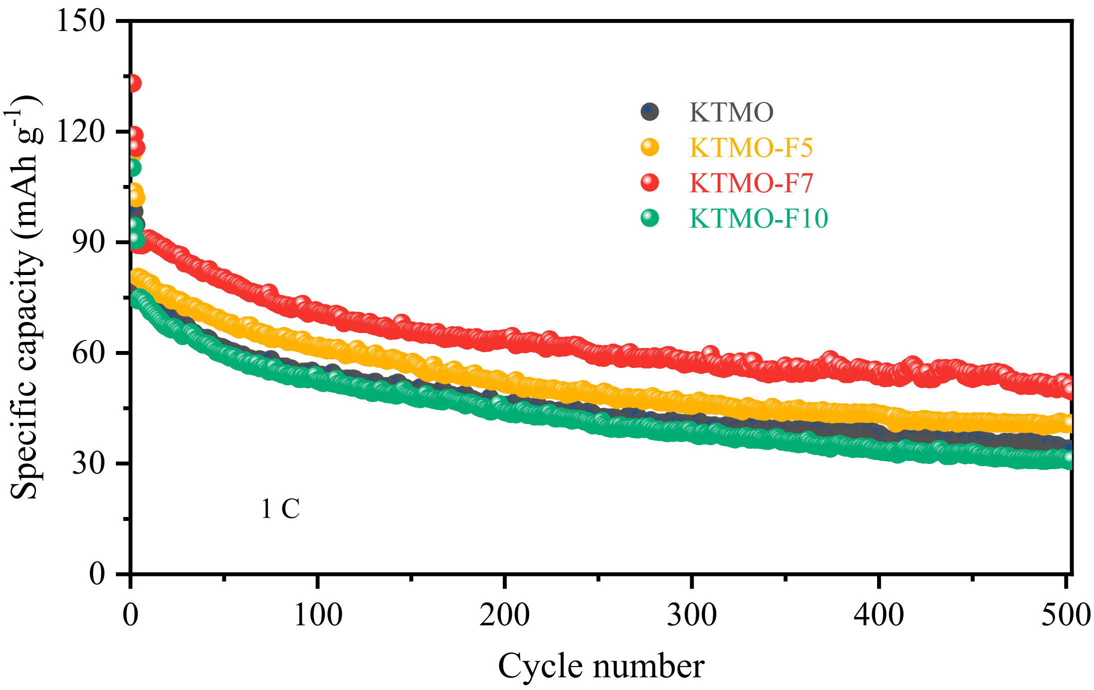

Fig. S8 Cycling performances at 1 C for 500 cycles.

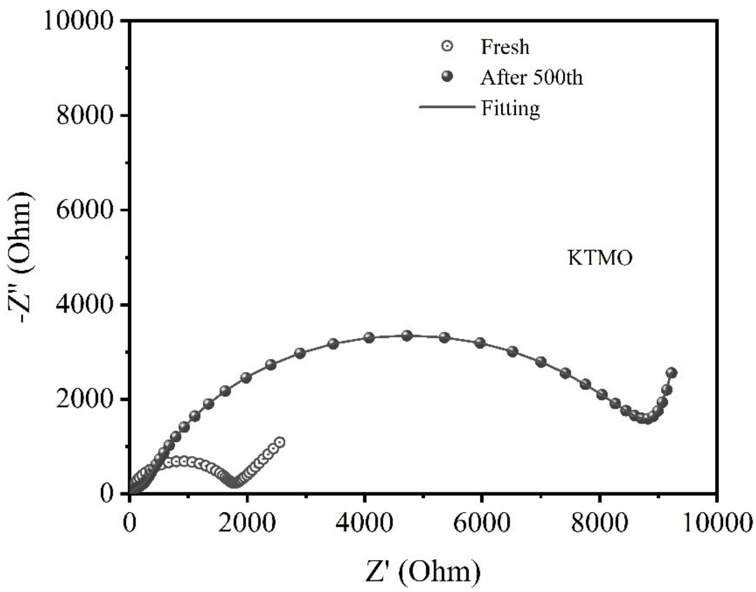

Fig. S9 Nyquist plots of KTMO in the initial state and after 500 cycles.

Table S1 Lattice parameters of KTMO-F5, KTMO-F7, and KTMO-F10 refined by the Rietveld method.

Samples	Space group	a (Å)	b (Å)	c (Å)	R_{wp} (%)
KTMO-F5	Ccmm	5.18	2.86	12.67	8.22
KTMO-F7	Ccmm	5.16	2.87	12.72	6.43
KTMO-F10	Ccmm	5.15	2.86	12.76	6.38

Table S2 pH values of $K_{0.6}Zn_{0.1}Ti_{0.05}Al_{0.05}Mn_{0.8}O_{2-x}F_x$ (x=0, 0.05, 0.07, 0.10).

Samples	KTMO	KTMO-F5	KTMO-F7	KTMO-F10
pH	11.21	11.38	11.67	11.75

Table S3 Area ratios of different valence elements in XPS.

Samples	Area ratio of Mn^{4+}/Mn^{3+}	Area ratio of surface O/lattice O
KTMO-F5	0.7164	0.0922
KTMO-F7	0.6371	0.1708
KTMO-F10	0.5808	1.3729

Table S4 Comparison of electrochemical capabilities between KTMO-F7 and reported materials.

Cathode materials	Discharge capacity/current density	Rate capacity/cycle/current density	[Ref]
$K_{0.44}Ni_{0.22}Mn_{0.78}O_2$	125.5/10	67/500/200	[1]
$K_{0.45}Ni_{0.8}Fe_{0.2}O_2$	106.2/20	77.3/100/20	[2]
$K_{0.45}Ni_{0.9}Mg_{0.1}O_2$	108/20	74.8/100/20	[3]
$K_{0.5}Mn_{0.72}Ni_{0.15}Co_{0.13}O_2$	82.5/10	85/100/50	[4]
$K_{0.6}Zn_{0.1}Ti_{0.05}Al_{0.05}Mn_{0.8}O_{1.93}F_{0.07}$	131.8/10	77/100/100	This work
$K_{0.45}Ni_{0.1}Co_{0.1}Al_{0.05}Mn_{0.8}O_2$	79/10	77/100/20	[5]
$K_{2/3}Mn_{7/9}Ni_{1/9}Ti_{1/9}O_{17/9}F_{1/9}$	54/500	91/50/100	[6]
$K_{0.6}Mn_{0.8}Ni_{0.1}Ti_{0.1}O_2$	118/10	88/100/200	[7]
$K_{0.45}Rb_{0.05}Mn_{0.85}Mg_{0.15}O_2$	108/20	98.2/200/200	[8]
$K_{0.37}Na_{0.3}Ni_{0.17}Co_{0.17}Mn_{0.66}O_2$	86.1/20	91.5/100/20	[9]

Table S5 Potassium-ion diffusion coefficients calculated from CV curves at different scan rates.

Sample	KTMO-F5	KTMO-F7	KTMO-F10
D_{K^+} (charging)	1.534×10^{-11} cm^2 s^{-1}	9.85×10^{-12} cm^2 s^{-1}	9.18×10^{-12} cm^2 s^{-1}
D_{K^+} (discharging)	1.19×10^{-11} cm^2 s^{-1}	1.9×10^{-11} cm^2 s^{-1}	9.0×10^{-12} cm^2 s^{-1}

Table S6 Potassium-ion diffusion coefficients calculated based on GITT measurements.

Sample	KTMO	KTMO-F5	KTMO-F7	KTMO-F10
D_{K^+} (cm^2 s^{-1})	4.05×10^{-12}	6.55×10^{-12}	1.29×10^{-11}	1.15×10^{-11}

Table S7 EIS test results of the four samples before/after 500 cycles.

Samples	*R*ct (Fresh)	*R*ct (After 500 cycles)
KTMO	1704 Ω	8809 Ω
KTMO-F5	1138 Ω	8451 Ω
KTMO-F7	901 Ω	4561 Ω
KTMO-F10	1172 Ω	5307 Ω

References

[1] X.Y. Zhang, Y.B. Yang, X.L. Qu, Z.X. Wei, G. Sun, K. Zheng, H.J. Yu, F. Du, Layered P2-Type $K_{0.44}Ni_{0.22}Mn_{0.78}O_2$ as a High-Performance Cathode for Potassium-Ion Batteries, Adv. Funct. Mater., 2019, 29, 1905679.

[2] C. Liu, S. Luo, H. Huang, X. Liu, Y. Zhai, Z. Wang, Fe-doped layered P3-type $K_{0.45}Mn_{1-x}Fe_xO_2$ ($x \leq 0.5$) as cathode materials for low-cost potassium-ion batteries, Chem. Eng. J., 2019, 378, 122167.

[3] C.L. liu, S.H. Luo, H.B. Huang, Y.C. Zhai, Z.W. Wang, Low-Cost Layered $K_{0.45}Mn_{0.9}Mg_{0.1}O_2$ as a High-Performance Cathode Material for K-Ion Batteries, ChemElectroChem., 2019, 6, 2308-2315.

[4] Q. Deng, F. Zheng, W. Zhong, Q. Pan, Y. Liu, Y. Li, G. Chen, Y. Li, C. Yang, M. Liu, P3-type $K_{0.5}Mn_{0.72}Ni_{0.15}Co_{0.13}O_2$ microspheres as cathode materials for high performance potassium-ion batteries, Chem. Eng. J., 2020, 392, 123735.

[5] R. Dang, N. Li, Y. Yang, K. Wu, Q. Li, Y.L. Lee, X. Liu, Z. Hu, X. Xiao, Designing advanced P3-type $K_{0.45}Ni_{0.1}Co_{0.1}Mn_{0.8}O_2$ and improving electrochemical performance via Al/Mg doping as a new cathode Material for potassium-ion batteries, J. Power Sources. 2020, 464, 228190.

[6] Y.-S. Xu, M.-Y. Qi, Q.-H. Zhang, F.-Q. Meng, Y.-N. Zhou, S.-J. Guo, Y.-G. Sun, L. Gu, B.-B. Chang, C.-T. Liu, A.-M. Cao, L.-J. Wan, Anion Doping for Layered Oxides with a Solid-Solution Reaction for Potassium-Ion Battery Cathodes, ACS Appl. Mater. Interfaces, 2022, 14, 13379-13387.

[7] Y.-S. Xu, Y.-N. Zhou, Q.-H. Zhang, M.-Y. Qi, S.-J. Guo, J.-M. Luo, Y.-G. Sun, L. Gu, A.-M. Cao, L.-J. Wan, Layered oxides with solid-solution reaction for high voltage potassium-ion batteries cathode, Chem. Eng. J. 2021, 412, 128735.

[8] Z.M. Caixiang, J.X. Hao, J. Zhou, X.Z. Yu, B.G. Lu, Interlayer-Engineering and Surface-Substituting Manganese-Based Self-Evolution for High-Performance Potassium Cathode. Adv. Energy Mater. 2023, 13, 2203126.

[9] C. Liu, S. Luo, H. Huang, Y. Zhai, Z. Wang, Influence of Na-substitution on the structure and electrochemical properties of layered oxides $K_{0.67}Ni_{0.17}Co_{0.17}Mn_{0.66}O_2$ cathode materials, Electrochim. Acta. 2018, 286, 114-122.